An injectable gelatin-based delivery platform mediated by guest-host complexation

Arbel M. Sisso

A thesis
submitted in partial fulfillment of the
requirements for the degree of

Master of Science in Bioengineering

University of Washington
2019

Committee:
Cole A. DeForest
Kelly Stevens

Program Authorized to Offer Degree:
Bioengineering

University of Washington

Abstract

An injectable gelatin-based delivery platform mediated by guest-host complexation

Arbel M. Sisso

Chair of the Supervisory Committee:
Assistant Professor Cole A. DeForest
Departments of Chemical Engineering and Bioengineering

Injectable hydrogel systems are beneficial for various biomedical applications, including drug or cell delivery carriers, and tissue engineering scaffolds. In this work, we describe the design and characterization of a shear-thinning hydrogel that undergoes a disassembly when shear forces are applied during injection and self-heals once shear forces are removed. This hydrogel is based on a mixture of cyclodextrin- and adamantane-modified gelatins, forming through a weak guest-host interaction between the hydrophobic cavities of the cyclodextrin host molecule and the hydrophobic adamantane guest. The shear-thinning and self-healing behavior of these gels was monitored in low and high strain range and the rheological analyses indicated the formation of shear-thinning gels compared with unmodified gelatin.

Table of Contents

List of Figures i
List of Schemes ii
A. Introduction 1
B. Experimental Section 6
B.1. Materials and Methods 6
B.2. β-CD-HDA Synthesis 6
B.3. Gelatin-Ad synthesis 8
B.4. Gelatin-β-CD synthesis 9
B.5. Deprotection of Gelatin-NH-BOC 9
B.6. Rheology Studies 10
B.6.1. Shear thinning properties 10
B.6.2. Comparative mechanical properties in hydrogels varying in G-Ad : G-bCD ratios 11
C. Results and Discussion 12
C.1. Chemical Modification of Gelatin 12
C.1.1. Synthesis of modified gelatin derivatives 12
C.1.2. Deprotection of primary amines of modified gelatin 15
C.1.3. Degree of functionalization of modified gelatin 18
C.2. Formation of hydrogels 19
C.3. Shear-thinning properties 21
C.4. Tunable mechanical properties 23
D. Conclusions 25
E. Bibliography 26

List of Figures

Figure 1. Deprotection of modified gelatin 17
Figure 2. Rapid association and dissociation of guest-host complementary bonds.....19
Figure 3. Liquid behavior of gelatin modified solution and a gel formation upon mixture.....20
Figure 4. Shear thinning behavior of synthesized hydrogels compared to unmodified gelatin. ...22
Figure 5. Storage and loss moduli of hydrogels in varying ratios of G-Ad : G-bCD.....23

Figure S1. $_1$H NMR of mono-6-OTs-β-CD.....31
Figure S2. $_1$H NMR of β-CD-HDA 32
Figure S3. Calibration curve for primary amine concentration.....33

List of Schemes

Scheme 1. β-Cyclodextrin-HDA synthesis 13
Scheme 2. Gelatin preparation for bioconjugation with β-CD/Ad 14
Scheme 3. Conjugation of β-CD/Ad to gelatin backbone 15
Scheme 4. Deprotection of Gelatin-NH-BOC-β-CD 16

A. Introduction

Hydrogels are hydrophilic macromolecular polymeric networks constructed of a variety of natural or synthetic building blocks or a mix thereof. They can retain a high concentration of water while preserving their structural integrity as a result of their crosslinking structure [1]. Hydrogels have been extensively researched for various biomedical applications including: delivery of therapeutic agents such as cells, drugs, proteins, and nucleic acids [3-6]; 3D dynamic cell culture support [7-10]; directing stem-cell fate [11, 12]; scaffolds for tissue engineering and regenerative medicine [13-15]; biomedical devices components [16]; bioadhesives [17]; and biosealants [18]. This is due to their many advantageous properties including biocompatibility, permeability to oxygen and nutrients, physical and mechanical properties that mimic the characteristics of the native extracellular matrix (ECM), and tunable physical, mechanical, and biological properties [2]. Biocompatibility and reactive chemistries are critical factors for selecting base materials that can be used to produce hydrogels for use in biomedical applications. Crosslinking type (physical *vs.* chemical) as well as crosslinking density, biodegradability, and biochemical properties are design criteria that will ultimately influence the mechanical, structural, and biological properties of the hydrogels [1, 2]. However, the clinical use of pre-formed hydrogels is limited since they require invasive surgical procedures for physical placement and retention of the therapeutic gel in the target site. This invasive procedure significantly increases risk of infection, complications, pain, patient discomfort, and medical care cost [19]. Injectable hydrogels are therefore beneficial to overcome such drawbacks, and as such they are particularly relevant in tissue engineering and therapeutic delivery applications [20-22]. In addition to the typical advantages of conventional hydrogels, injectable gels readily take the shape of irregular cavities while providing a minimally invasive module of delivery. The materials can be applied using a syringe or a catheter as they

undergo a sol-to-gel transition at the desired target site. Furthermore, various therapeutic agents such as proteins, drugs, and cells can be mixed into the precursor solution prior to injection to afford simple incorporation into the hydrogel. Therefore, injectable hydrogels are of increasing interest in the field of tissue engineering and therapeutic delivery [20-22].

One common approach for engineering an injectable hydrogel is to design liquid precursors that gel *in situ* during/after injection through either chemical or physical cross-linking mechanisms. Though this approach has proven beneficial in many systems, there are potential drawbacks in requiring an external stimulus to initiate gelation process or a multi-barrel syringe system for incorporation of reactive components together during injection. Another important variable in this process is sol-gel transition time; a rapid cross-linking of the hydrogel may result in clogging of the catheter or syringe prior to the deployment of the hydrogel, whereas a lagging cross-linking process may lead to material dissipation upon injection prior to setting. Moreover, release of unreacted precursors outside of the target zone due to slow gelation raises the risk of emboli formation and off-site cytotoxicity [20-22].

To overcome the challenges of *in situ* cross-linking systems, hydrogels with the ability to flow under application of shear stress (i.e., shear-thinning) and reform upon removal of stress (i.e., self-healing) have gained popularity. The most common cross-linking route for the formation of shear-thinning hydrogels is through physical self-assembly. Shear-thinning systems vary according to the self-assembly mechanism on which they are based on, achieved through numerous noncovalent chemical interactions (e.g., hydrogen bonds, electrostatic interactions, hydrophobic interactions). Though each individual bond is weak, cumulatively they can result in formation of materials with high structural integrity [21, 23].

One example of a particularly interesting application for injectable shear-thinning hydrogels is cardiac regeneration following a myocardial infarction (MI) event [24]. MI occurs as a result of an occlusion or blockage of a coronary artery that provides oxygenated blood to the heart muscle itself. Tissue located downstream to the blockage will become ischemic, and prolonged lack of oxygen will result in irreversible necrosis of heart muscle. Being one of the least regenerative organs in the body, loss of heart tissue results in fibrotic scar formation that can cause significant deficit of contractile force and ultimately lead to heart failure (HF).

With cardiovascular diseases being a leading cause of death and the number one healthcare cost globally, significant effort has been put into developing techniques to promote cardiac regeneration [24-26]. Researchers have sought after therapeutic strategies dedicated to improving myocardial regeneration and restoration of function including direct injection of cardiomyocytes (CM) [27], stem cells [28], biomolecules [29, 30], and chemokines [31]. While demonstrating some positive effect, these techniques suffer from significant impediments such as nonspecific delivery, low cell survival, and insignificant engraftment rate in the desired targeted region [32].

Efforts of tissue engineering researchers have focused on overcoming these drawbacks by applying injectable biomaterials designed to protect the therapeutic cargo from degradation, improve targeted engraftment, and increase cell survival during and post injection [32, 33]. Moreover, increased engraftment efficiencies allow for fewer cells to be used to achieve a therapeutic effect, resulting in a significant cost reduction.

One strategy for the development of such shear-thinning hydrogels utilized polyzwitterionic polycarboxybetaine that form shear-thinning micro-gel pellets providing tunable storage moduli [34]. Another approach utilized alginate-based hydrogels that demonstrate inherent shear-thinning behavior as a result of physical electrostatic crosslinking with Ca^{+2} ions. These have

been reported to improve cell viability during injection compared to injection of cells in phosphate-buffered saline (PBS) [35, 36]. In a recent study, alginate hydrogels were investigated as an injectable cell-free support of the left ventricle in a clinical trial for patients with advanced HF. While the treatment improved the exercise capacity of the treated patients, 8.6% of patients who received the hydrogel injection died within 30 days post-injection whereas no fatalities occurred within the control group at the same time [37]. A different system was designed by modifying hyaluronic acid (HA) hydrogels to incorporate guest-host interactions. The hydrogels were used to encapsulate rat endothelial progenitor cells followed by injection to MI rat model and resulted in enhancement of vascular density at the infarct [38]. A shear-thinning, protein-based hydrogel with cell-adhesive domains was reported to improve induced pluripotent stem cells derived endothelial cells (iPSC-EC) viability during the injection process by protecting the cells from mechanical forces within the needle [39].

When exploring materials that can potentially provide a suitable environment for cardiac cells, we turned to the structure of the natural cardiac ECM, where the most abundant protein is collagen [40, 41]. Though we expected a collagen-based material to provide appropriate physiochemical cues to support long term cell culture, collagen in its natural form is highly viscous and difficult to handle. Moreover, intact collagen has been reported to induce immunogenic response in some patients [42]. Therefore, we hypothesized that utilizing gelatin, a biocompatible and non-immunogenetic protein originating from denatured collagen with potentially tunable and easy-to-use properties, would promote cell survival when used as a cell scaffold.

Gelatin is a protein cured from collagen that has previously been reported to have biocompatible, biodegradable, non-immunogenic, cell-integration properties [43] and therefore

presents a leading candidate to produce a cardiac scaffold. However, gelatin is a liquid at body temperature, and therefore cannot be used as a stable scaffold *in vivo*; chemical modifications are required to provide stability to its structure and enhance its mechanical properties while avoiding rapid degradation upon exposure to host-tissue [43]. Many chemical and enzymatic modifications have been utilized to alter gelatin's mechanical properties (e.g., glutaraldehyde, carbodiimide (EDAC), transglutaminase, methacrylation) [44-48]. Though these approaches can yield stable materials that have been beneficial for cell culture and drug delivery, there has yet to be developed a method that affords a stimuli-free, by-product free, single-barrel injection of an *in situ* self-healing gelatin.

In this study, we sought to develop a gelatin-based shear-thinning injectable platform for minimally invasive therapeutic delivery. Towards this, we functionalized the gelatin backbone with complementary association domains whose physical interaction could be disrupted with mild shear force. We sought to employ guest-host chemistry based on physical hydrophobic bonding between a cyclic cup-shaped host (i.e., β-cyclodextrin) and a complimentary guest molecule (i.e., adamantane). These moieties were conjugated onto the gelatin backbone using EDAC/NHS chemistry; rapid association and dissociation of the guest-host bonds upon application of low- and high-shear respectively resulted in the formation of a shear-thinning injectable gelatin-based platform that can potentially be used as a minimally invasive drug and cell delivery module.

B. Experimental Section

B.1. Materials and Methods

Gelatin type A (porcine skin, ~275 bloom, 40-50kDa), β-cyclodextrin (β-CD), 1-adamantylamine hydrochloride (Ad), *p*-Toluenesulfonyl Chloride (TsCl), *o*-Phthaldialdehyde (OPA), and 1,6-Hexanediamine (HDA) were purchased from Acros Organics (Fair Lawn, NJ). Sodium Hydroxide (NaOH), Acetone, Acetonitrile, Glycine, Sodium Tetraborate, Ethanol, and Anhydrous Diethyl Ether were purchased from Fischer Scientific (Fair Lawn, NJ). Ammonium Chloride was purchased from JT Baker (Phillipsburg, NJ). Anhydrous Dimethyl sulfoxide (DMSO), and di-tert-butyl dicarbonate (BOC) were purchased from Alfa Aesar (Tewksbury, MA). *N*-hydroxysuccinimide (NHS), 2-mercaptoethanol, and N,N-dimethyl formamide (DMF) were purchased from Sigma-Aldrich (St. Louis, MO). 1-Ethyl-3-(3-dimethylaminopropyl) carbodiimide (EDAC) was purchased from AK Scientific (Union City, CA). d*6*-DMSO was purchased from Cambridge isotope laboratories (Andover, MA). Hydrochloric acid (HCl) 12M was purchased from Avantoc (Center Valley, PA). All chemicals were used as received, unless stated otherwise.

UV analysis was performed with SpectraMax M5 UV-VIS spectrophotometer (Molecular Devices, San Jose, CA). ^{1}H NMR spectra performed in DMSO-d*6* using Avance 300 MHz instrument (Bruker, Billerica, MA). Freeze-drying of the polymer derivatives occurred by means of FreeZone 2.5plus lyophilizer (Labconco, Kansas City, MO). Rheology experiments performed on Physica MCR301 Rheometer (Anton Paar, Graz, Austria).

B.2. β-CD-HDA Synthesis

6-(6-aminohexyl)amino-6-deoxy-β-cyclodextrin (β-CD-HDA) synthesis was performed by adaptation of previously reported similar syntheses [49-51]. A round-bottom flask was charged with β-CD (1 equiv, 20 g, 17.62 mmol) and double-distilled water (DDW; 150 ml), and cooled

on ice to 0°C for 1 hour. NaOH (3.1 equiv, 2.2 g, 55 mmol) was dissolved in 6.67 ml of DDW and added dropwise. By the end of the addition of NaOH, the solution turned completely homogeneous and clear. The suspension was stirred for 30 minutes at room temperature. TsCl (1.25 equiv, 4.2 g, 22 mmol) was dissolved in minimal acetonitrile (10 ml) and added dropwise to β-CD suspension. Immediate precipitation was observed upon TsCl addition. The suspension was stirred at room temperature for two hours. pH was adjusted to 8-8.5 by addition of approximately 10gr of solid ammonium chloride (NH_4Cl) and suspension was cooled at 4°C overnight. Precipitate was collected by glass filter (M funnel) using vacuum pump and rinsed with DDW (400 ml), washed by acetone (300 ml), and dried under vacuum to afford the intermediate 6-o-monotosyl-6-deoxy-β-cyclodextrin [5.09 g, 3.948 mmol, 22.4% (molar)] as a white powder. ^{1}H NMR (DMSO-d*6*) spectrum is presented in *figure S1*, δ = 7.76 (d, 2H), 7.44 (d, 2H), 5.89-5.56 (m, 14H), 4.84 (s, 5H), 4.78 (s, 2H), 4.12-4.55 (m, 9H), 3.8-3.42 (m, 28H), 3.41-3.06 (m, overlaps with H_2O), 2.42 (s, 3H).

A round-bottom flask was charged with 6-o-monotosyl-6-deoxy-β-cyclodextrin (1 equiv, 5 gr, 3.878 mmol) and dissolved in 10 ml DMF. 1,6-hexanediamine (HDA; 45 equiv, 20 gr, 172.1 mmol) was dissolved in 15 ml DMF separately and then added to the round-bottom flask (overall 25 ml DMF). Reaction was carried out under nitrogen conditions for 20 hours with a reflux condensing setup and a temperature-controlled silicon oil bath (80°C). Reaction flask was uninstalled and cooled to room temperature for one hour. Product was precipitated using cold acetone (500 ml, 4 °C) and collected by glass filter (M funnel) using vacuum pump. Precipitate was re-dissolved in DMF (25 ml) and then reprecipitated with acetone (500 ml). This process was repeated 3 times. Precipitate was washed by cold diethyl ether (200 ml, 4 °C) twice and filtered by vacuum on M glass funnel as a pale-yellow slurry. Product was dried under vacuum

for two hours to afford the final β-CD-HDA product [3.06 gr, 2.48 mmol, 63.9% (molar)] as a light brown powder. ^{1}H NMR (DMSO-d*6*) spectrum is presented in *figure S2,* δ = 5.71 (br s, 14H), 4.83 (br s, 7H), 4.46 (br s, 6H), 3.79-3.5 (m, 28H), 3.5-3.17 (m, overlaps with H_2O), 1.6-1.08 (m, 12H).

B.3. Gelatin-Ad synthesis

Gelatin-adamantane synthesis was performed by adaptation of previously reported synthesis describing conjugation of 2-aminoethyl methacrylate (AEMA) to carboxylic acid side chains of Gelatin [52]. Gelatin A (5 g, 1.455 mmol amine of lysine and hydroxylysine [55], 4.255 mmol carboxylic acids [56], 1 equiv) was dissolved in 50 ml anhydrous DMSO at 55°C under nitrogen atmosphere and reflux conditions. After obtaining a homogeneous solution, BOC (635.1 mg, 2.91 mmol, 2 equiv) was added and the reaction mixture was stirred for 80 min. Molar excess of BOC was considered with respect to free amino groups of gelatin based on a content of 0.291 mmol free amine groups per gram of gelatin type A [55]. EDAC (991 mg, 6.383 mmol, 1.5 equiv) was added and the solution was stirred for 5 minutes. NHS (979.5 mg, 8.51 mmol, 2 equiv) was included in the reaction mixture followed by stirring for 45 minutes. 1-Adamantylamine (Ad; 835.7 mg, 5.525 mmol, 1.3 equiv) was added and the reaction occurred overnight (20 hrs.) while stirring at 55°C under nitrogen atmosphere with reflux conditions. Molar excess of EDAC, NHS, and Ad were considered in respect to carboxylic acid side chains based on a content of 0.851 mmol carboxylic acid groups per gram gelatin type A [56]. Mixture was precipitated in a tenfold excess (500 ml) of cold acetone and filtered on a glass filter (M). The residue was dissolved in minimal DDW at 50°C and transferred to dialysis membranes (MWCO: 3500 Da) against DDW for 48 hours at 42°C. Dialysis product was frozen and lyophilized for 48 hours and a light-yellow spongy material was received (1.746g).

B.4. Gelatin-β-CD synthesis

Gelatin-β-Cyclodextrin synthesis was performed by adaptation of Gelatin-Ad synthesis, with the single change of addition of 1.3 equiv β-CD-HDA instead of 1.3 equiv 1-adamantylamine. A light-brown powder was recovered (3.524 g product per 5 g of gelatin). An additional synthesis was conducted with 3.5 equiv β-CD-HDA (385 mg product per 1 g of gelatin).

B.5. Deprotection of Gelatin-NH-BOC

BOC deprotection was performed by adaptation of previously reported procedure [52]. Gelatin-NH-BOC (100 mg/ml) was dissolved in DDW. Next, 0.5 v/v% of an aqueous HCl solution (12M) was added. The quantity of protective groups removed from modified gelatin was determined indirectly by evaluating the difference between the amine content in gelatin prior to and after BOC deprotection. Amine concentration was determined spectrometrically using *o*-phthaldialdehyde (OPA). The reaction between primary amines and OPA resulted in the formation of isoindol chromophores possessing a maximum absorbance λ_{max} at 340 nm. The deprotection reaction proceeded over several days at 4 °C and the quantification of the amine concentrations was relative to a calibration curve based on glycine standards (*figure S3*). Solution A was prepared by dissolving 5 mg OPA in 2.5 ml ethanol and diluting the mixture to 15 ml using DDW. 30 ml of borate buffer pH=10 were prepared separately by mixing 13ml of NaOH 0.1M solution and 17ml of Sodium Tetraborate solution in DDW at 0.05M. Solution B was prepared by adding 15 µl 2-mercapto-ethanol to previously prepared 30 ml borate buffer. The two solutions were then combined to prepare a 40 ml stock solution made of 10 ml solution A and 30 ml solution B. Samples at concentration of 100 mg/ml were diluted to 1 mg/ml with DDW prior to measurement. 100 µl of natural or modified gelatin samples (1 mg/ml) at different time points of the deprotection reaction were added to a 96-well microplate. 200 µl stock solution was added to each well (overall 300 µl in each well) and absorbance at λ_{max} = 340 nm

was measured two minutes after addition of stock solution to the samples. Blank (i.e., mixture with water instead of gelatin) measurements were then subtracted from the sample measurements. Similar measurements were performed with glycine (0.03 – 0.5 mM) standards to obtain a calibration curve (*figure S3*). Calculation of the amount of free amine groups remaining after the modification, enabled the determination of the deprotection degree of Gelatin-NH-BOC. Once the absorbance measurement reached the measurement of the unmodified gelatin, the samples were taken out to dialysis for 48 hours (MWCO: 3500 Da) at 42 °C against DDW, then frozen, and lyophilized before any further use.

B.6. Rheology Studies

B.6.1.Shear thinning properties

The hydrogels were formed on the rheometer plate by mixing varying volume ratios of Gelatin-β-CD (G-bCD) in DDW (400 mg/ml) with Gelatin-Ad (G-Ad) in DDW (400 mg/ml) between parallel plates (8 mm diameter). An overall volume of 40 µl was used to form hydrogels with 0.5 mm thickness. Silicon oil was used to seal the sample and prevent drying. The storage and loss moduli (G’ and G”, respectively) were recorded at constant angular frequency (10 rad/s) with cyclic strain varying from low and high strain (10% and 400%, respectively) at the temperature of 25 °C. Unmodified gelatin of similar storage modulus (70 mg/ml) was used as a control measurement. Angular frequency, low, and high strain were determined according to angular frequency sweep and strain amplitude sweep, respectively, below the limit of the linear viscoelastic region (LVE). LVE was determined by the curve of the G' function, where it shows a constant value (or, plateau value).

B.6.2.Oscillatory time sweeps of hydrogels varying in G-Ad : G-bCD ratios

G’ and G” of hydrogels were measured in hydrogels formed with varying volume ratios of G-Ad : G-bCD. Individual solutions contained 400mg/ml G-Ad or G-bCD in DDW. Measurements were conducted 30 minutes after mixture of the solutions together on the rheometer plate. The measurement spanned over 5 minutes at an angular frequency of 10 rad/sec and oscillatory strain of 10%, at temperature of 25 °C. Two hydrogels of each formation were measured, and an average of the results over time with a standard deviation is presented in the results.

.

C. Results and Discussion

C.1. Chemical Modification of Gelatin

C.1.1. Synthesis of modified gelatin derivatives

The aim of the present study is the development of novel shear-thinning gelatin derivatives that upon mixing allow the formation of an injectable gel, to be used as a therapeutic cargo delivery. Gelatin contains many chemical functionalities in the side chains of the different amino acids which can be exploited for a bioconjugation reaction. It contains amine functionalities in the side chains of lysine and hydroxylysine; carboxylic acids in the side chains of glutamic and aspartic acid; and hydroxyl functionalities in the side chains of serine, threonine and hydroxylysine [53]. While most gelatin modification strategies reported in literature use the primary amines as a handle to introduce functionalities [54], we have decided to use the carboxylic acid functionalities as they are more abundant than primary amine functionalities (7.7% to 3.3% respectively) [53]. In order to introduce β-cyclodextrin (β-CD) as a pendant moiety on the gelatin backbone, β-CD was modified to contain a primary amine by addition of a single 1,6-hexanediamine (HDA) chain to the cyclic shaped β-CD carbohydrate. This was achieved by initial mono-tosylation of β-CD, according to previously reported synthesis, under basic aqueous conditions [49-51]. Chemical structure of product was verified using ^{1}H NMR (*figure S1*). Then, an excess of HDA was reacted with the previous product under dry N_2 conditions, in anhydrous DMF at 80 °C overnight. ^{1}H NMR was used to confirm the structure of the product β-CD-HDA (*figure S2, Scheme 1*). The modification of carboxylic acid functionalities present in the glutamate and aspartate side chains of the gelatin was carried out using conventional carbodiimide coupling in anhydrous DMSO under dry N_2 conditions at 55°C overnight. First, the primary amine side chains of gelatin were protected using di-*tert*-butyl dicarbonate (BOC) in order to prevent cross-linking between activated carboxylic acid side

chains with primary amine side chains. Then, 1-Ethyl-3-(3-dimethylaminopropyl) carbodiimide (EDAC) was introduced, followed by addition of *N*-Hydroxysuccinimide (NHS) to stabilize the activated carboxylic acid groups (*Scheme 2*). Using a primary amine as a nucleophile (either 1-adamantylamine or β-CD-HDA), a nucleophilic substitution was realized, and a stable amide bond was formed. As a result, either Adamantane (Ad) or β-CD were introduced into the gelatin backbone (*Scheme 3*).

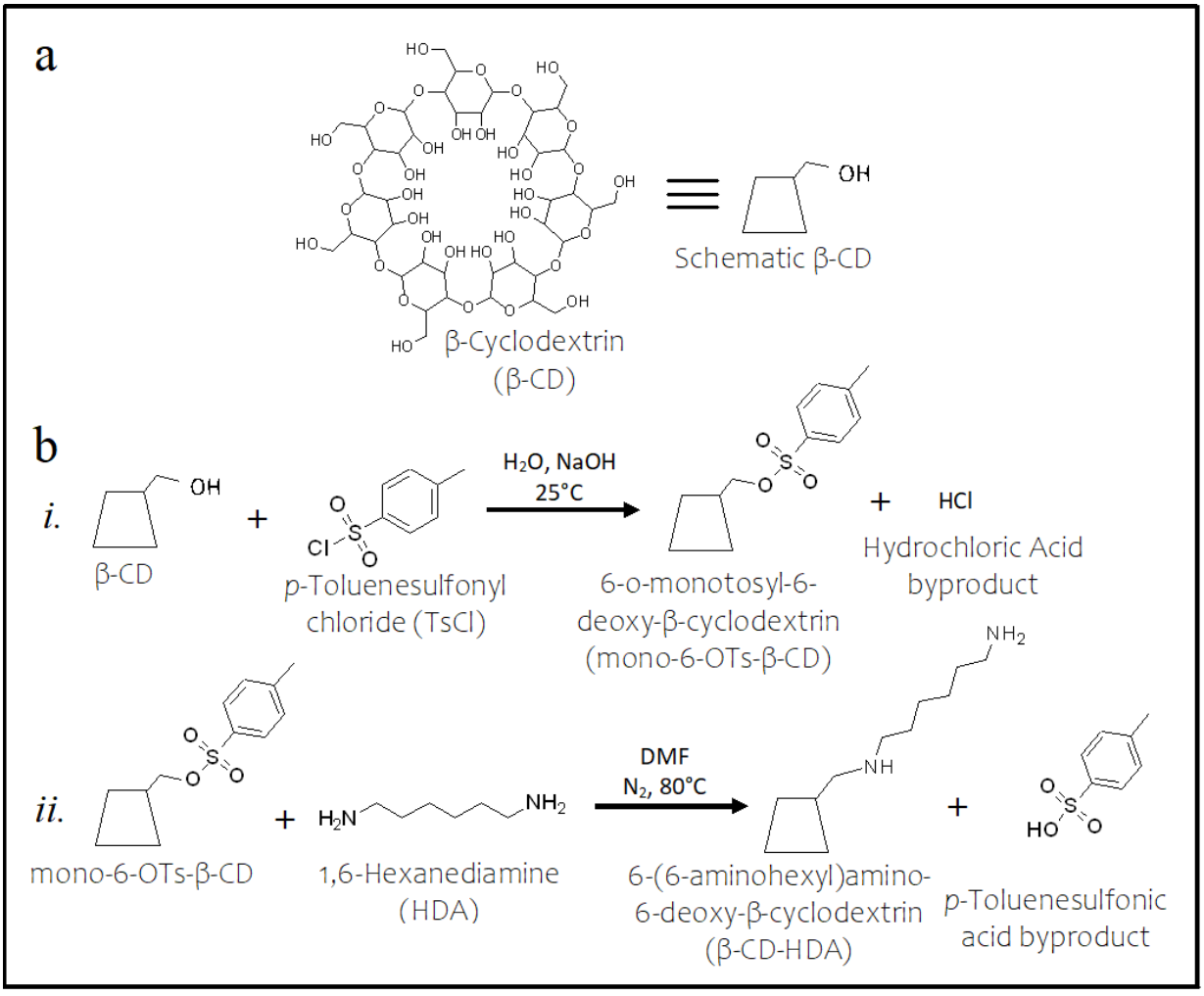

Scheme 1. β-Cyclodextrin-HDA synthesis

(a) Schematic representation of β-Cyclodextrin (β-CD). (b) *i.* First step of alcohol activation using TsCl. Single tosylation was achieved by dropwise addition of TsCl to a basic aqueous solution containing β-CD. *ii.* Excess of HDA was introduced to the dry mono-6-OTs-β-CD under anhydrous conditions for overnight reaction at 80°C. Final product β-CD-HDA was achieved as a white powder.

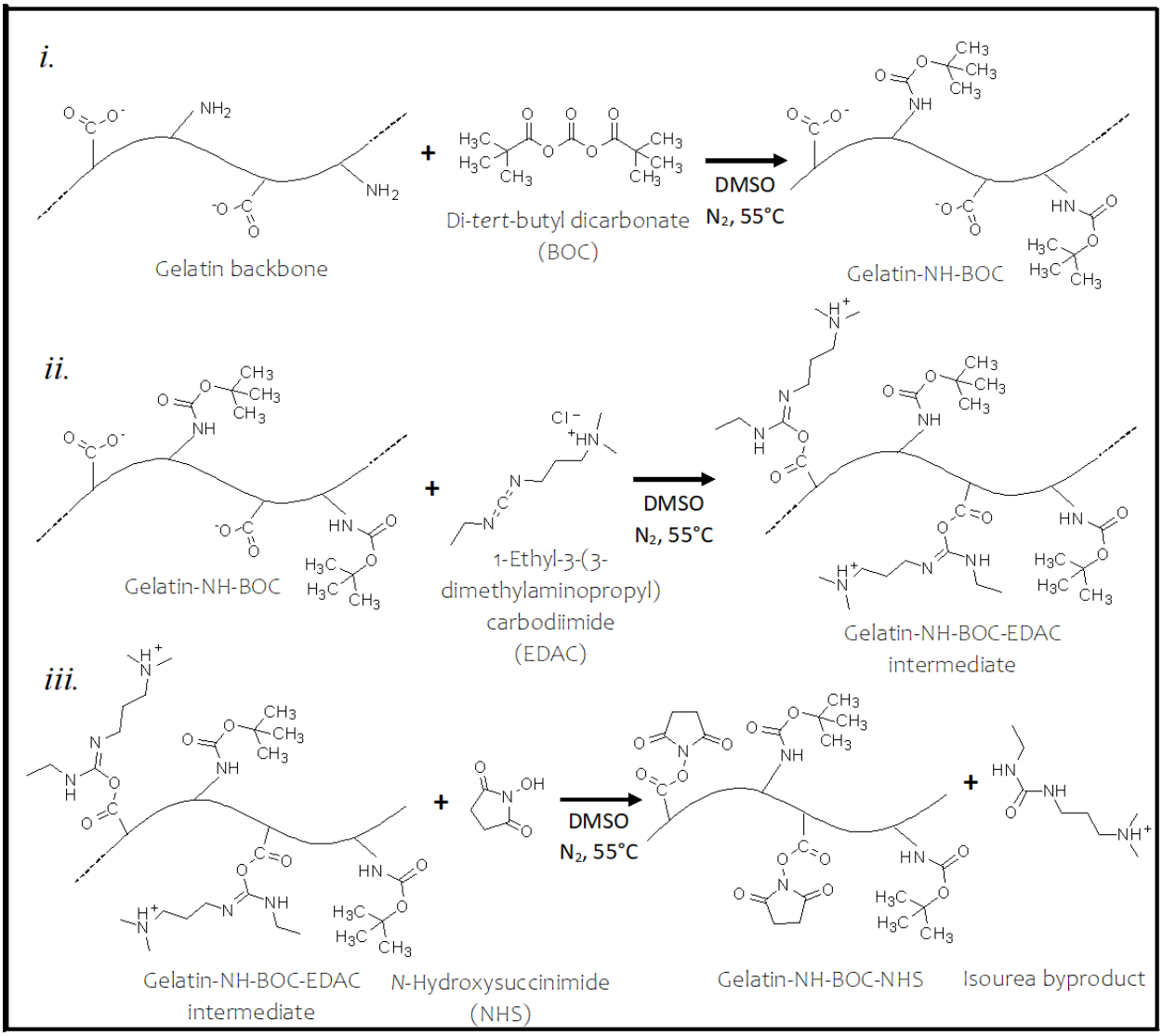

Scheme 2. Gelatin preparation for bioconjugation with β-CD/Ad

i. A schematic representation of Gelatin is presented by a backbone line with the amine and carboxylic acid side chains. Initial step is protection of primary amines *via* BOC protecting group for the prevention of chemical crosslinking of the gelatin. *ii*. Second, EDAC is introduced to form an active intermediate. *iii*. Then, NHS is added to replace the highly active EDAC intermediate and result in formation of slightly more stable intermediate. This may be readily reacted with primary amine containing molecules for the formation of a stable amide bond between the activated carboxylic acid and the primary amine introduced.

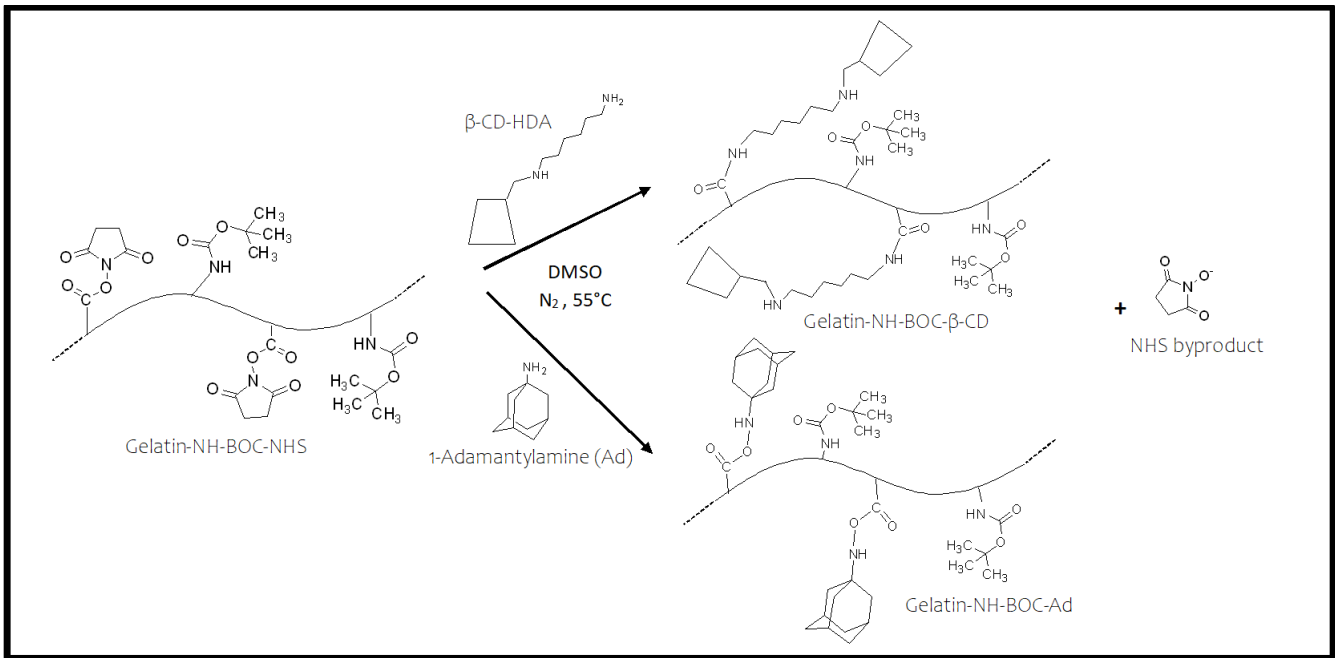

Scheme 3. Conjugation of β-CD/Ad to gelatin backbone

Gelatin-NH-BOC-NHS is reacted with either β-CD-HDA or 1-Adamantylamine under dry DMSO and N_2 conditions. An amide bond is formed between the activated carboxylic acid on the gelatin backbone and the primary amine of 1-Adamantylamine/β-CD-HDA.

C.1.2. Deprotection of primary amines of modified gelatin

The quantity of incorporated NH-BOC protective groups in gelatin derivatives was determined by evaluating the difference between the amine content in modified compared to unmodified gelatin (*figure 1*). As a result of primary amine protection, less amines in gelatin are available for reaction with OPA resulting in lower absorbance values at 340 nm. The difference in absorbance is proportional with the quantity of protected amines. The deprotection of primary amines was achieved by addition of 0.5% v/v HCl 12M (*Scheme 4*) and evaluated spectrometrically using OPA. As deprotection advances over time, more primary amines become available to react with OPA, which results in higher absorbance values at 340 nm. The difference in absorbance is proportional with the quantity of deprotected amines. Unmodified gelatin was subjected to the same acid treatment, as a control measurement. In *figure 1a* a comparison

between gelatin-NH-BOC and unmodified gelatin is presented. Both acid-treated and not-treated samples were measured for the free primary amine content over the course of 500 hours.

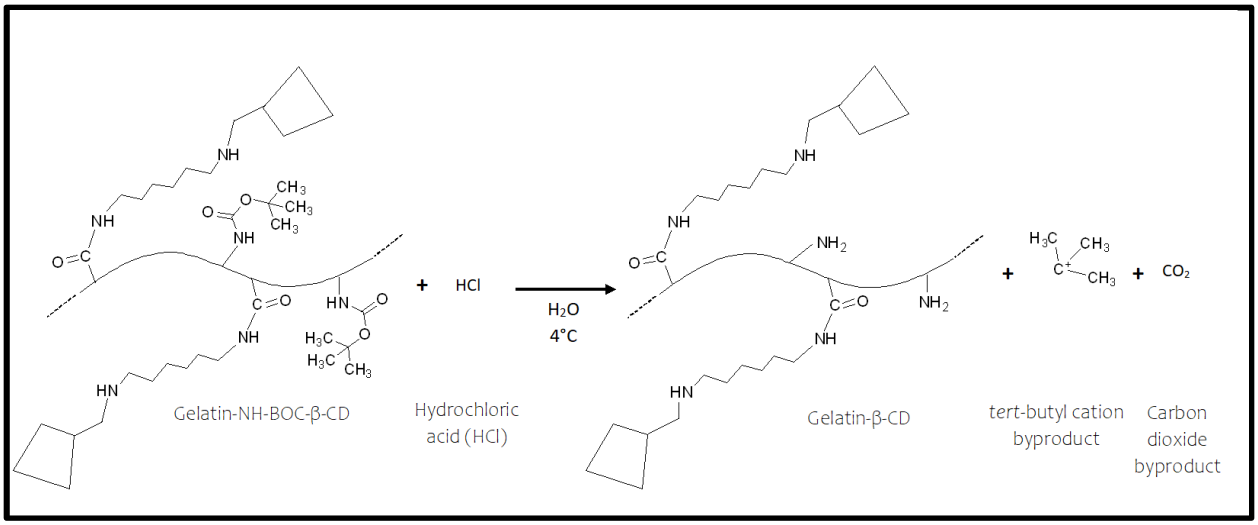

Scheme 4. Deprotection of Gelatin-NH-BOC-β-CD

Gelatin-NH-BOC-β-CD and Gelatin-NH-BOC-Ad were subjected to acid treatment until BOC deprotection was complete. Here, we depict the chemical scheme of deprotection of Gelatin-NH-BOC-β-CD.

Acid-treated natural gelatin does not show an increase in amine content compared to untreated gelatin over the course of the treatment, indicating no acid-catalyzed gelatin backbone degradation occurs. *Figure 1b and 1c* present the comparison between unmodified gelatin and gelatin modified with Ad and β-CD, respectively. Once the absorbance of the treated samples had reached the absorbance level of unmodified gelatin (indicated with a red mark), samples were taken to dialysis and ultimately lyophilized. Untreated samples have not shown significant increase in absorbance and hence free-amine content, confirming a stable protection, and justifying the requirement of acid addition to achieve deprotection. A calibration curve of amine concentration (mM) to absorbance was constructed using glycine standards of increasing concentrations (*figure S3*). According to the linear correlation observed, the natural gelatin we used in our experiments contains 0.291 mmol_NH_2 / gr_gelatin (*figure S3*, average of 0.48

absorbance). This finding is in line with previous primary amine measurements of gelatin type A which reported 0.284-0.288 mmol_NH_2 / gr_gelatin [55].

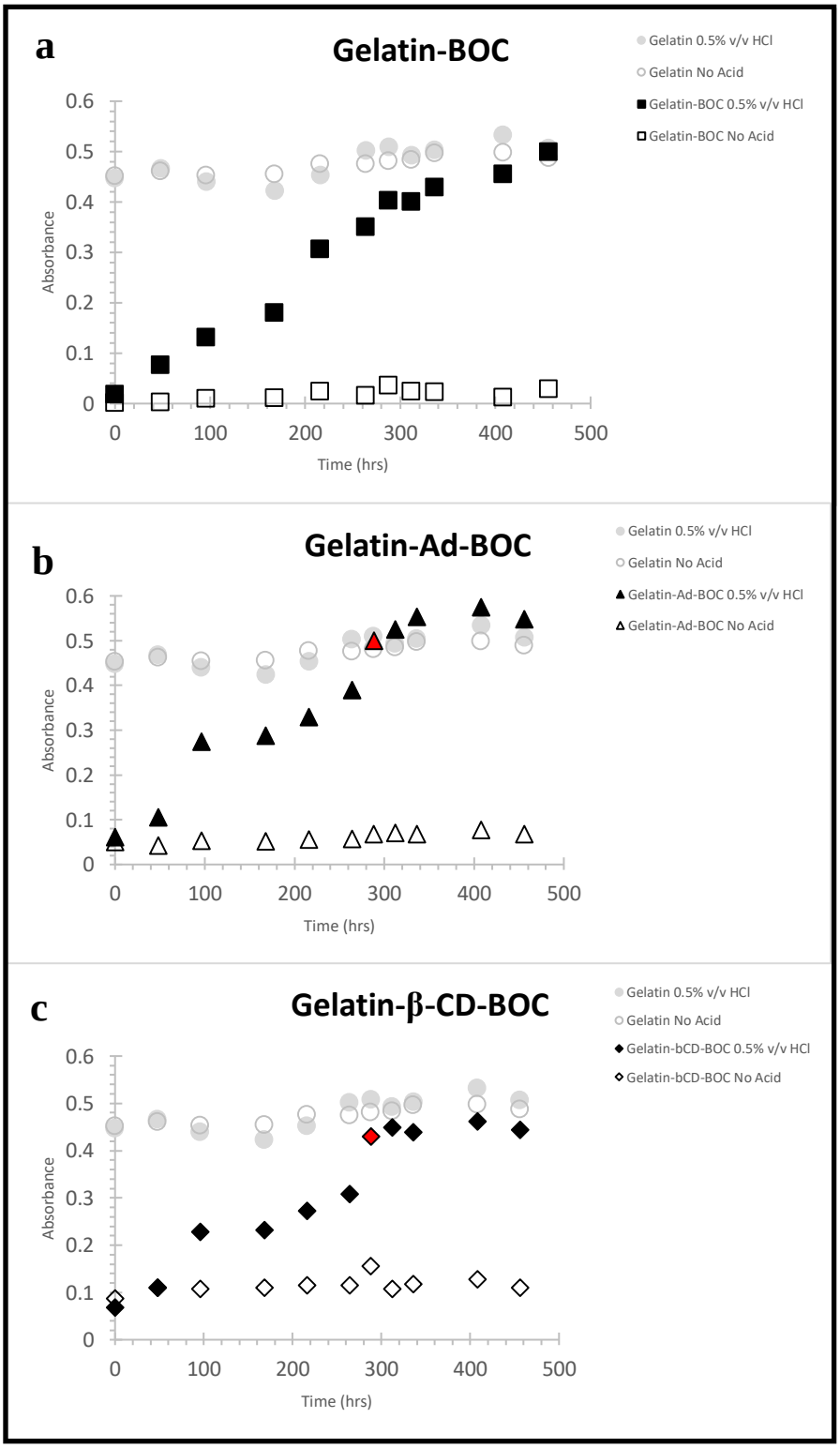

Figure 1. Deprotection of modified gelatin

Primary amines of lysine and hydroxylysine side chains in the gelatin were protected using BOC. Deprotection process was conducted using addition of 0.5% v/v HCl 12M. Process was monitored using OPA reagent for detection of free primary amines over time *via* absorbance at 340nm. Both acid-treated (full) and untreated samples (empty) were measured for amine content.

(a) Unmodified gelatin (gray circles) and gelatin modified with BOC only (black square),

(b) Gelatin-Ad-BOC (black triangle), and

(c) Gelatin-β-CD-BOC (black diamond).

C.1.3. Degree of functionalization of modified gelatin

As discussed earlier, gelatin is a naturally derived material, composed of a variety of proteins with a wide molecular weight distribution and an amino acid composition that may vary from batch-to-batch. As such, the degree to which the carboxylic acid side chains of the gelatin were functionalized is very difficult to determine. The ^{1}H NMR spectrum of gelatin is very complex as varying amino acids are connected through amide linkages.

In order to determine a reference signal to standardize measurements of area under curve or integral, it was essential to attribute a peak to a component that remains chemically inert during the modification process. The signal at 7.5 ppm ascribed to the resonance of amino acid phenylalanine was selected as a reference signal. The resonance contributed by Ad was absent on the spectrum of Ad-modified gelatin compared to the unmodified gelatin. Therefore, a degree of functionalization (DoF) was not calculated for Gelatin-Ad. However, a single significant peak, that varied from the unmodified gelatin, was observed in samples functionalized with β-CD.

When synthesizing gelatin modified β-CD, varying syntheses were carried out, each with a different molar ratio between gelatin and β-CD-HDA (1:1.3, 1:3.5). However, during evaluation of ^{1}H NMR spectra, there were no significant differences in the standardized area under curve at the β-CD peak at 4.83 ppm.

This finding may indicate that all carboxylic acid side chains were functionalized when synthesized with initial ratio of 1:1.3, or that the resonance in this peak does not indicate the degree of functionalization of gelatin with β-CD. Unfortunately, no other distinct peaks were found that could be used as indicators for DoF of gelatin with β-CD and therefore successful functionalization is indicated by shear-thinning behavior that is demonstrated using rheology measurements.

C.2. Formation of hydrogels

The hydrogel was formed via the reversible complexation of the guest-host coupling between Ad and β-CD when a solution of β-CD-modified gelatin was mixed with Ad-modified gelatin solution as schematically showed in *figure 2*.

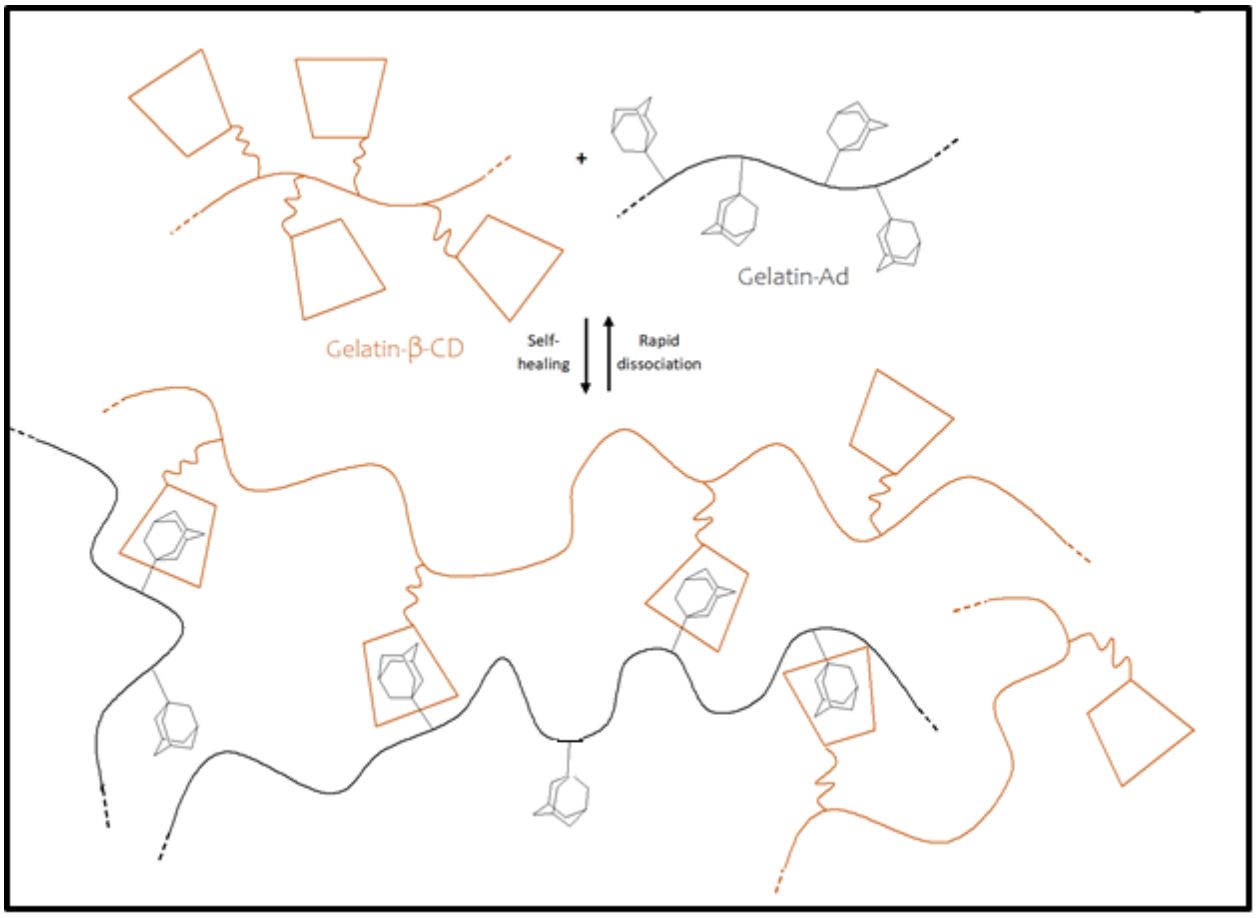

Figure 2. Rapid association and dissociation of guest-host complementary bonds

Upon mixture of Gelatin-Ad and Gelatin-β-CD together, a hydrogel forms as a result of transient hydrophobic bond formation between the host moiety (β-CD) and the guest moiety (Ad). When high shear is applied, the gel becomes a viscous liquid, allowing for flow of material.

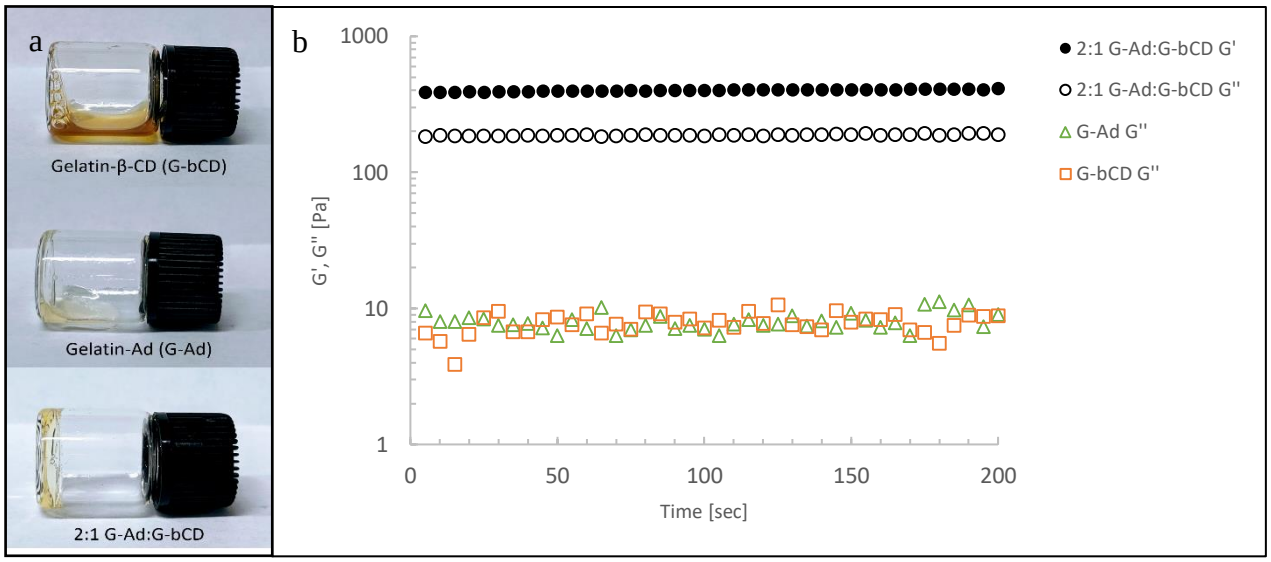

Figure 3. Liquid behavior of separate gelatin modified solutions and a gel formation upon mixture

(a) Inversion test of Ad modified gelatin (G-Ad; 400 mg/ml, top), β-CD modified gelatin (G-bCD; 400 mg/ml, middle), and a 2:1 volume ratio mixture of the two components together (400 mg/ml, bottom). (b) Oscillatory time sweeps of individual components G-Ad (400 mg/ml), G-bCD (400 mg/ml), and a 2:1 volume ratio mixture of the two components together (400 mg/ml); Storage modulus (G′, filled symbols) and loss modulus (G′′, empty symbols) measured at 25°C, 10% strain, and angular velocity of 10rad/sec.

Interestingly, each separate modified gelatin solution (400 mg/ml) was in liquid state at room temperature, while upon mixture of the two solutions, hydrogel formation occurred. A qualitative inversion test was performed to demonstrate this phenomenon (*figure 3a*). Storage and loss moduli were measured for each individual solution, and demonstrated a behavior of a viscous liquid, indicated by absence of storage modulus and a low value of loss modulus as depicted in *figure 3b*. Whereas, a mixture of the two solutions together in a volume ratio of 2:1 G-Ad : G-bCD showed an increase in both storage and loss moduli, and a behavior of an elastic gel, indicated by storage modulus values higher than loss modulus values (*figure 3b*).

C.3. Shear-thinning properties

The design of a guest–host assembly system that is based on dynamically reversible bonds, formed hydrogels that exhibit shear-thinning and self-healing characteristics. To demonstrate these properties, that are especially desired in injectable delivery systems, hydrogels of varying in Ad to β-CD ratios were subjected to cycles of high oscillatory strain (400%) followed by low oscillatory strain (10%). Unmodified gelatin of similar storage modulus was used as a control in these rheology measurements. During periods of high oscillatory strain, the materials demonstrated a clear reduction in storage modulus and an almost immediate gel-sol transition, indicated by a viscous flow behavior of G''>G'.

Upon removal of high strain conditions, an elastic solid-like behavior occurred (G'>G''), and a gradual recovery to the initial storage modulus was observed (*figure 4*). Similar self-healing mechanical characteristics were observed regardless of the number of cycles performed. These results indicate that the materials are capable of recovery following high-shear events such as injection, that will potentially allow for retention of the matrix with the intercalated therapeutic cargo at the desired target site.

Unmodified gelatin control did not demonstrate shear thinning behavior under the same rheology conditions. This is demonstrated by the continuous occurring of a gel structure regardless of oscillatory strain, indicated by elastic behavior of G'>G'' (*figure 4*).

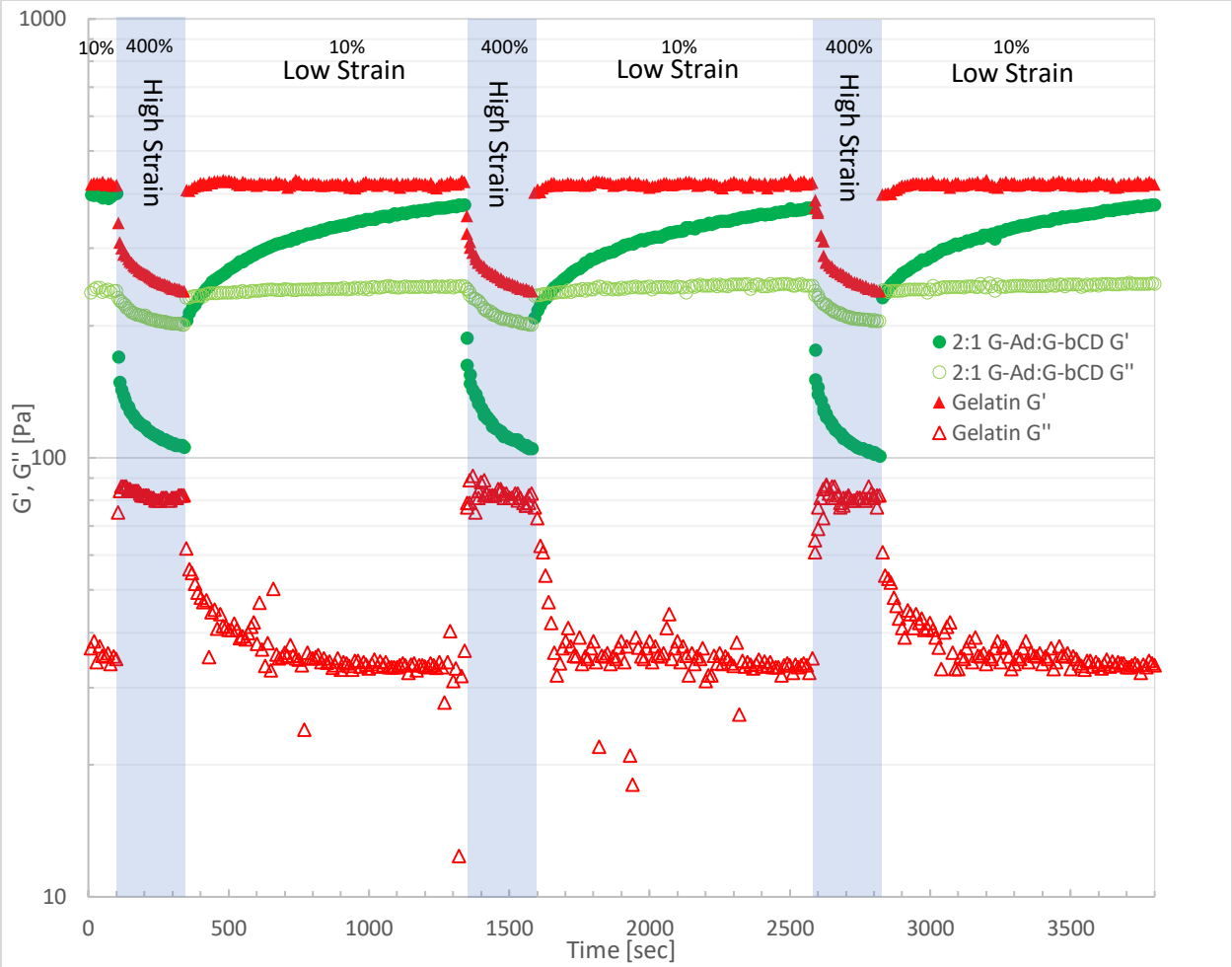

Figure 4. Shear thinning behavior of newly synthesized hydrogels compared to unmodified gelatin

Rheology measurements of G′ (storage modulus; filled symbols) and G′′ (loss modulus; empty symbols) at cycles of high oscillatory strain (400%, blue background) followed by low oscillatory strain (10%, white background) of hydrogel composed of 2:1 volume ratio of G-Ad:G-bCD (400 mg/ml; green) and unmodified gelatin (70 mg/ml; red); 25 °C, 10 rad/sec.

C.4. Tunable mechanical properties

Storage and loss moduli measurements of hydrogels with varying volume ratios of G-Ad : G-bCD were conducted in order to determine the change in behavior according to quantity of host molecules compared to guest molecules. Concentration of each individual solution was 400mg/ml, keeping the total amount of dry material constant upon mixture.

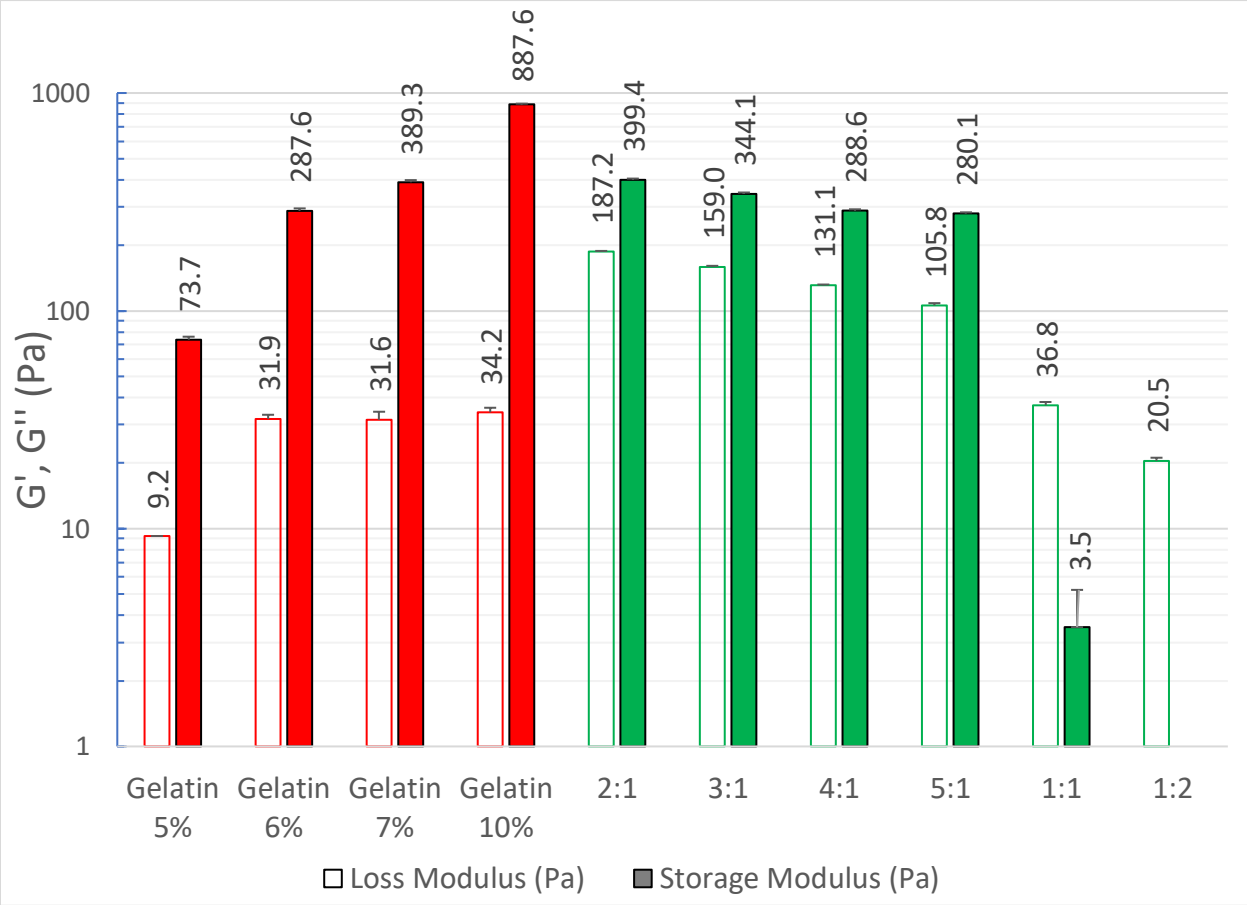

Figure 5. Storage and loss moduli of hydrogels varying ratios of G-Ad : G-bCD

Values of G′ (filled bars), G′′ (empty bars) of unmodified gelatin with varying w/v % (left, red), compared with hydrogels of varying G-Ad : G-bCD volume ratios (right, green). Each individual solution (G-Ad, G-bCD) was in concentration of 400 mg/ml. Error bars indicate standard deviation of measurements over the course of the test, for overall two gel samples of each type.

The oscillatory time sweeps measurements presented in *figure 5* indicate that a volume ratio of 2:1 G-Ad : G-bCD (400 mg/ml) results in the formation of a gel with the highest storage modulus out of the varying ratios measured (~400 Pa). As the G-Ad : G-bCD ratio increases, a reduction in storage modulus is observed, when a 4:1 and 5:1 ratio obtain very similar loss and storage moduli. All hydrogels presented a shear-thinning and self-healing behavior (data not shown). A decrease in ratio under 2:1 does not result in a formation of a gel, as indicated by behavior of G”>G’ or an absence of storage modulus. These results indicate that a formation of a stable hydrogel is dependent on the quantity of guest compared to host moieties present in the gel. The ability to tune the mechanical properties of the gel, by controlling the ratio of host to guest and therefore controlling the cross-linking density, is an important feature that may allow a formation of a hydrogel with the desired mechanical properties suitable to the relevant application.

D. Conclusions

The most common strategy to produce injectable hydrogels is to develop a system that can easily be injected as a liquid, followed by the rapid formation of a solid gel network. In this study, a shear-thinning and self-healing hydrogel was synthesized and analyzed for its mechanical properties. The self-healing properties of this system was generated by the formation of inclusion complex between the hydrophobic cavity of β-cyclodextrin attached to the gelatin backbone and a hydrophobic adamantane attached to the gelatin backbone. The rheological analyses confirmed the recoverability of the shear-thinning material. Since these hydrogels are based on natural polymers which are safe to use and biodegradable, they have the potential to be used in and cell- or drug-delivery, as well as for tissue engineering applications. However, further in-depth studies are required to determine degradability, cytotoxicity, drug release rate, protection of cells from shear-forces during injection, and cell retention degree post-injection.

Future modification of the material to retain higher storage modulus may include a secondary cross-linking method, or an addition of guest and host moieties to the gelatin backbone by utilizing both carboxylic acids and primary amines in the gelatin.

E. Bibliography

1. Hoffman, A. (2012). Hydrogels for biomedical applications. *Advanced Drug Delivery Reviews, 64*, 18-23.

2. Chai, Q., Jiao, Y., & Yu, X. (2017). Hydrogels for Biomedical Applications: Their Characteristics and the Mechanisms behind Them. *Gels, 3*(1), 6.

3. Youngblood, R., Truong, N., Segura, T., & Shea, L. (2018). It's All in the Delivery: Designing Hydrogels for Cell and Non-viral Gene Therapies. *Molecular Therapy*, *26*(9), 2087-2106.

4. Hoare, T., & Kohane, D. (2008). Hydrogels in drug delivery: Progress and challenges. *Polymer*, *49*(8), 1993-2007.

5. Ruskowitz, E., Comerford, M., Badeau, B., & Deforest, C. (2019). Logical stimuli-triggered delivery of small molecules from hydrogel biomaterials. *Biomaterials Science*, *7*(2), 542-546.

6. Gawade, P., Shadish, J., Badeau, B., & DeForest, C. (2019). Logic-Based Delivery of Site-Specifically Modified Proteins from Environmentally Responsive Hydrogel Biomaterials. *Advanced Materials*, 1902462.

7. Caliari, S., & Burdick, J. (2016). A practical guide to hydrogels for cell culture. *Nature Methods, 13(5)*, 405-414.

8. Shadish, J., Benuska, G., & DeForest, C. (2019). Bioactive site-specifically modified proteins for 4D patterning of gel biomaterials. *Nature Materials*.

9. Kloxin, A., Lewis, K., Deforest, C., Seedorf, G., Tibbitt, M., Balasubramaniam, V., & Anseth, K. (2012). Responsive culture platform to examine the influence of microenvironmental geometry on cell function in 3D. *Integrative Biology (United Kingdom), 4*(12), 1540-1549.

10. Uto, K., Tsui, J., DeForest, C., & Kim, D.-H. (2017). Dynamically Tunable Cell Culture Platforms for Tissue Engineering and Mechanobiology. *Progress in polymer science, 65*, 53-82.

11. Deforest, C., & Tirrell, D. (2015). A photoreversible protein-patterning approach for guiding stem cell fate in three-dimensional gels. *Nature Materials, 14*(5), 523-531.

12. DeForest, C., & Anseth, K. (2012). Advances in Bioactive Hydrogels to Probe and Direct Cell Fate. *Annual Review of Chemical and Biomolecular Engineering, 3*(1), 421-444.

13. Saul, J., & Williams, D. (2013). Hydrogels in Regenerative Medicine. In J. Saul, & D. Williams, *Handbook of Polymer Applications in Medicine and Medical Devices* (279-302). Elsevier Inc.

14. El-Sherbiny, I., & Yacoub, M. (2013). Hydrogel scaffolds for tissue engineering: Progress and challenges. *Global Cardiology Science and Practice, 2013*(3), 316-342.

15. Arakawa, C., Badeau, B., Zheng, Y., & DeForest, C. (2017). Multicellular Vascularized Engineered Tissues through User-Programmable Biomaterial Photodegradation. *Advanced Materials, 29*(37), 1703156.

16. Caló, E., & Khutoryanskiy, V. (2015). Biomedical applications of hydrogels: A review of patents and commercial products. *European Polymer Journal*, *65*, 252-267.

17. Ghobril, C., & Grinstaff, M. (2015). The chemistry and engineering of polymeric hydrogel adhesives for wound closure: A tutorial. *Chemical Society Reviews, 44(7)*, 1820-1835.

18. Annabi, N., Yue, K., Tamayol, A., & Khademhosseini, A. (2015). Elastic sealants for surgical applications. *European Journal of Pharmaceutics and Biopharmaceutics, 95*, 27-39.

19. Doenst, T., Diab, M., Sponholz, C., Bauer, M., & Färber, G. (2017). The opportunities and limitations of minimally invasive cardiac surgery. *Deutsches Arzteblatt International, 114(46)*, 777-784.

20. Thambi, T., Li, Y., & Lee, D. (2017). Injectable hydrogels for sustained release of therapeutic agents. *Journal of Controlled Release*, *267*, 57-66.

21. Guvendiren, M., Lu, H., & Burdick, J. (2012). Shear-thinning hydrogels for biomedical applications. *Soft Matter, 8(2)*, 260-272.

22. Lee, J. (2018). Injectable hydrogels delivering therapeutic agents for disease treatment and tissue engineering. *Biomaterials Research, 22*(1), 22-27.

23. Zhang, S. (2002). Emerging biological materials through molecular self-assembly. *Biotechnology Advances*, *20*(5-6), 321-339.

24. Laflamme, M., & Murry, C. (2011,). Heart regeneration. *Nature*, *473*, 326-335.

25. Bertero, A., & Murry, C. (2018). Hallmarks of cardiac regeneration. *Nature Reviews Cardiology, 15(10)*, 579-580.

26. Sangeetha, V., & W, C. (2018). Cardiac Regeneration. *Circulation Research, 123*(1), 24-26.

27. Chong, J., Yang, X., Don, C., Minami, E., Liu, Y., Weyers, J., Murry, C. (2014). Human embryonic-stem-cell-derived cardiomyocytes regenerate non-human primate hearts. *Nature*, *510*(7504), 273-277.

28. Amado, L., Saliaris, A., Schuleri, K., St. John, M., Xie, J.-S., Cattaneo, S., Hare, J. (2005). Cardiac repair with intramyocardial injection of allogeneic mesenchymal stem cells after myocardial infarction. *Proceedings of the National Academy of Sciences*, *102*(32), 11474-11479.

29. Rebouças, J., Santos-Magalhães, N., & Formiga, F. (2016). Cardiac Regeneration using Growth Factors: Advances and Challenges. *Arquivos Brasileiros de Cardiologia*, *107*(3), 271–275.

30. Korf-Klingebiel, M., Reboll, M., Klede, S., Brod, T., Pich, A., Polten, F., & Wollert, K. (2015). Myeloid-derived growth factor (C19orf10) mediates cardiac repair following myocardial infarction. *Nature Medicine, 21*(2), 140-149.

31. Dobaczewski, M., & Frangogiannis, N. (2008). Chemokines in myocardial infarction: Translating basic research into clinical medicine. *Future Cardiology, 4*(4), 347-351.

32. Roche, E., Hastings, C., Lewin, S., Shvartsman, D., Brudno, Y., Vasilyev, N., Mooney, D. (2014). Comparison of biomaterial delivery vehicles for improving acute retention of stem cells in the infarcted heart. *Biomaterials, 35*(25), 6850-6858.

33. Janani, A., & Sridhar Skylab, R. (2014). Injectable hydrogel for cardiac tissue engineering. *International Journal of ChemTech Research, 6*(3), 2233-2236.

34. Sinclair, A., O'Kelly, M., Bai, T., Hung, H., Jain, P., & Jiang, S. (2018). Self-Healing Zwitterionic Microgels as a Versatile Platform for Malleable Cell Constructs and Injectable Therapies. *Advanced Materials, 30*(39). 1803087.

35. Aguado, B., Mulyasasmita, W., Su, J., Lampe, K., & Heilshorn, S. (2011). Improving Viability of Stem Cells During Syringe Needle Flow Through the Design of Hydrogel Cell Carriers. *Tissue Engineering Part A, 18*(7-8), 806-815.

36. Ruvinov, E., & Cohen, S. (2016). Alginate biomaterial for the treatment of myocardial infarction: Progress, translational strategies, and clinical outlook. From ocean algae to patient bedside. *Advanced Drug Delivery Reviews, 96*, 54-76.

37. Anker, S., Coats, J., Cristian, G., Dragomir, D., Pusineri, E., Piredda, M., Mann, D. (2015). A prospective comparison of alginate-hydrogel with standard medical therapy to determine impact on functional capacity and clinical outcomes in patients with advanced heart failure (AUGMENT-HF trial). *European heart journal*, *36*(34), 2297–2309.

38. Gaffey, A., Chen, M., Venkataraman, C., Trubelja, A., Rodell, C., Dinh, P., & Atluri, P. (2015). Injectable shear-thinning hydrogels used to deliver endothelial progenitor cells, enhance cell engraftment, and improve ischemic myocardium. *Journal of Thoracic and Cardiovascular Surgery, 150*(5), 1268-1277.

39. Wong Po Foo, C., Lee, J., Mulyasasmita, W., Parisi-Amon, A., & Heilshorn, S. (2009). Two-component protein-engineered physical hydrogels for cell encapsulation. *Proceedings of the National Academy of Sciences, 106*(52), 22067-22072.

40. Engler, A., Carag-Krieger, C., Johnson, C., Raab, M., Tang, H.-Y., Speicher, D., Discher, D. (2008). Embryonic cardiomyocytes beat best on a matrix with heart-like elasticity: scar-like rigidity inhibits beating. *Journal of Cell Science, 121*(22), 3794-3802.

41. Lockhart, M., Wirrig, E., Phelps, A., & Wessels, A. (2011). Extracellular matrix and heart development. *Birth Defects Research Part A - Clinical and Molecular Teratology, 91(6)*, 535-550.

42. Lynn, A., Yannas, I., & Bonfield, W. (2004). Antigenicity and immunogenicity of collagen. *Journal of Biomedical Materials Research - Part B Applied Biomaterials, 71(2),* 343-354.

43. Nikkhah, M., Akbari, M., Paul, A., Memic, A., Dolatshahi-Pirouz, A., & Khademhosseini, A. (2016). Gelatin-based biomaterials for tissue engineering and stem cell bioengineering. In Neves, N., M., & Reis, R., L. *Biomaterials from Nature for Advanced Devices and Therapies* (1st Ed., p. 37-51). Hooken, NJ: John Wiley & Sons, Inc.

44. Kuijpers, A., Engbers, G., Krijgsveld, J., Zaat, S., Dankert, J., & Feijen, J. (2000). Crosslinking and characterisation of gelatin matrices for biomedical applications. *Journal of Biomaterials Science-Polymer, 11*, 225-243.

45. Sung, H., Huang, D., Chang, W., Huang, R., & Hsu, J. (1999). Evaluation of gelatin hydrogel crosslinked with various crosslinking agents as bioadhesives: In vitro study. *Journal of Biomedical Materials Research, 46*, 520-530.

46. Nikkhah, M., Eshak, N., Zorlutuna, P., Annabi, N., Castello, M., Kim, K., Khademhosseini, A. (2012). Directed endothelial cell morphogenesis in micropatterned gelatin methacrylate hydrogels. *Biomaterials, 33*(35), 9009-9018.

47. Nichol, J., Koshy, S., Bae, H., Hwang, C., Yamanlar, S., & Khademhosseini, A. (2010). Cell-laden microengineered gelatin methacrylate hydrogels. *Biomaterials, 31*(21), 5536-5544.

48. Benton, J., DeForest, C., Vivekanandan, V., & Anseth, K. (2009). Photocrosslinking of Gelatin Macromers to Synthesize Porous Hydrogels That Promote Valvular Interstitial Cell Function. *Tissue Engineering Part A, 15*(11), 3221-3230.

49. Fetter RC, Salek JS, Sikorski CT, Kumaravel G, a. (1990). Cooperative Binding by Aggregated Mono-6-(alkylamino)-/3-cyclodextrins. *Journal of American Chemical Soceity, 112*(10), 3860-3868.

50. Kaya, E., & Mathias, L. (2010). Synthesis and characterization of physical crosslinking systems based on cyclodextrin inclusion/host-guest complexation. *Journal of Polymer Science, Part A: Polymer Chemistry, 48*(3), 581-592.

51. Rodell, C., Kaminski, A., & Burdick, J. (2013). Rational design of network properties in guest-host assembled and shear-thinning hyaluronic acid hydrogels. *Biomacromolecules, 14*(11), 4125-4134.

52. Van Nieuwenhove, I., Stubbe, B., Graulus, G., Van Vlierberghe, S., & Dubruel, P. (2014). Protein functionalization revised: N-tert-butoxycarbonylation as an elegant tool to circumvent protein crosslinking. *Macromolecular Rapid Communications, 35*(15), 1351-1355.

53. Mark, J. (2009). *Polymer Data Handbook* (2nd Ed.). Oxford, NY: Oxford University Press.

54. Van Hoorick, J., Tytgat, L., Dobos, A., Ottevaere, H., Van Erps, J., Thienpont, H., & Van Vlierberghe, S. (2019). (Photo-)crosslinkable gelatins for biofabrication applications. *Acta Biomaterialia*.

55. Kale, R., & Bajaj, A. (2010). Ultraviolet Spectrophotometric Method for Determination of Gelatin Crosslinking in the Presence of Amino Groups. *Journal of Young Pharmacists. 2* (1), 90-94.

56. Rose, P., I. (1987). Gelatin. In Mark, H., F., & Kroschwitz, J., I. *Encyclopedia of Polymer Science and Engineering* (2nd Ed., Vol. 7, p. 502) New York, NY: John Wiley & Sons, Inc.

Appendix and Supplementary

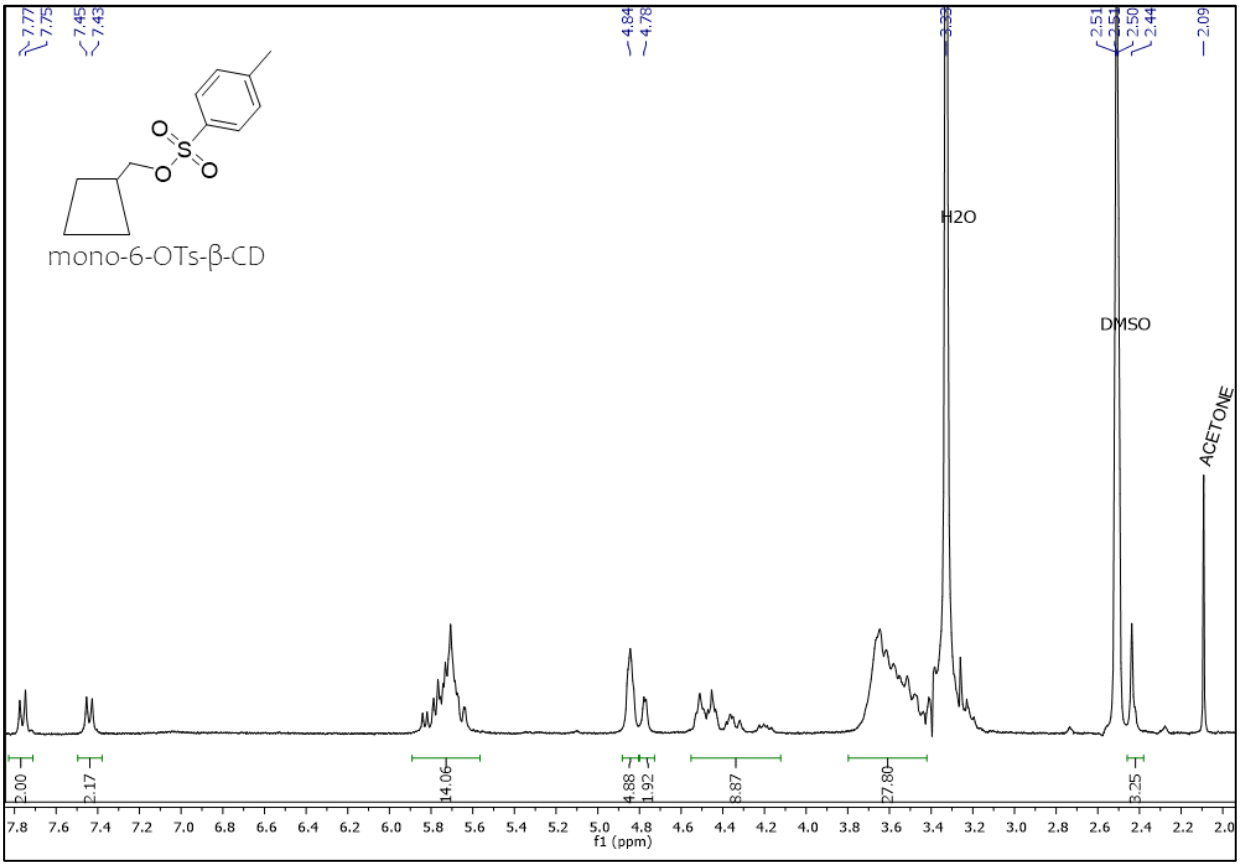

Figure S1. ^{1}H NMR of mono-6-OTs-β-CD

Mono-6-OTs-β-CD chemical structure was verified using ^{1}H NMR in DMSO-d6. Structure was compared with previously reported syntheses and NMR analyses [49, 50]. δ = 7.76 (d, 2H), 7.44 (d, 2H), 5.89-5.56 (m, 14H), 4.84 (s, 5H), 4.78 (s, 2H), 4.12-4.55 (m, 9H), 3.8-3.42 (m, 28H), 3.41-3.06 (m, overlaps with H2O), 2.42 (s, 3H). Other peaks are a result of solvents used during reaction or DMSO-d6 and are noted on the spectrum.

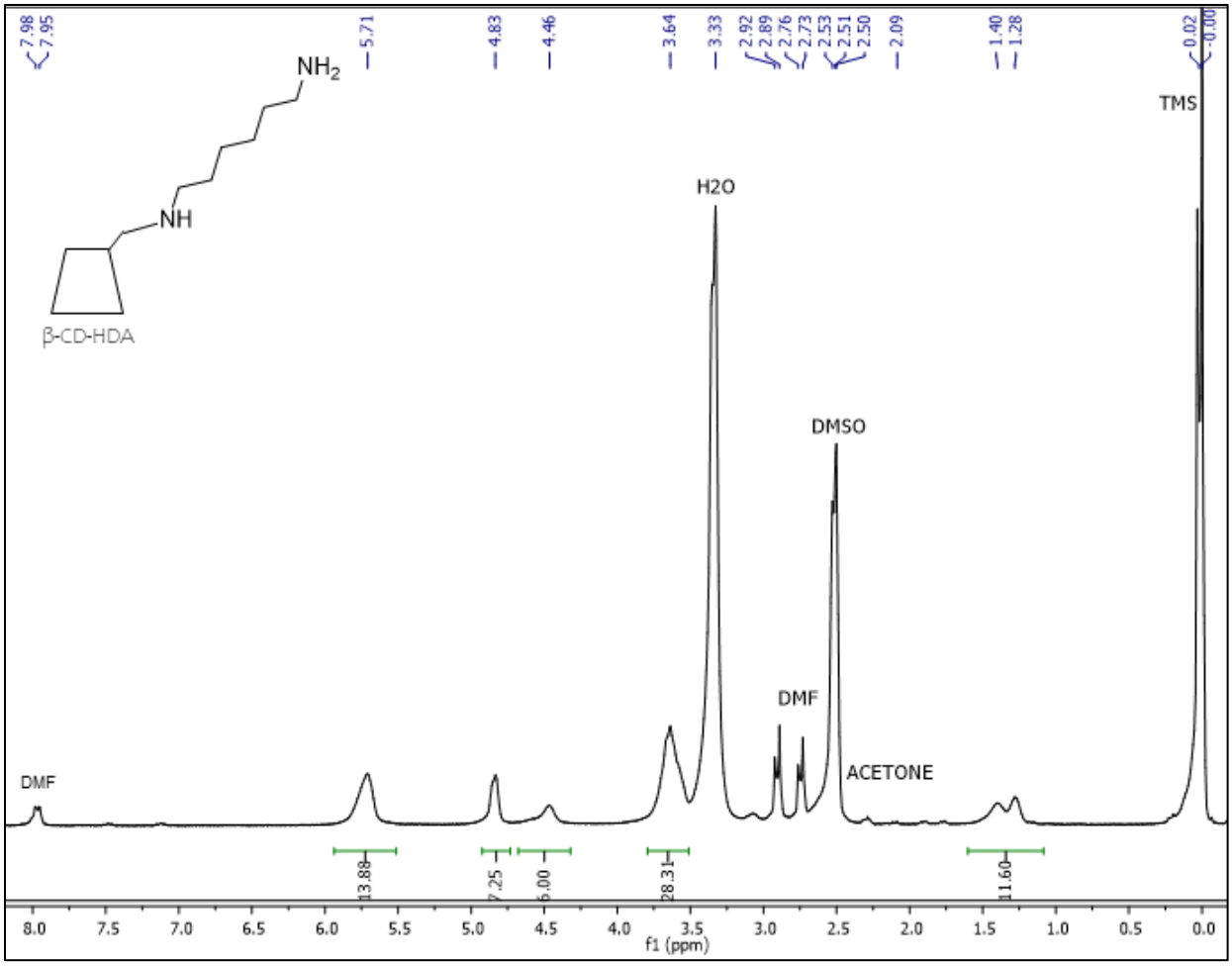

Figure S2. ^{1}H NMR of β-CD-HDA

β-CD-HDA chemical structure was verified using ^{1}H NMR in DMSO-d6. Structure was compared with previously reported syntheses and NMR analyses [50, 51]. δ = 5.71 (br s, 14H), 4.83 (br s, 7H), 4.46 (br s, 6H), 3.79-3.5 (m, 28H), 3.5-3.17 (m, overlaps with H_2O), 1.6-1.08 (m, 12H). Other peaks are a result of solvents used during reaction or DMSO-d6 and are noted on the spectrum.

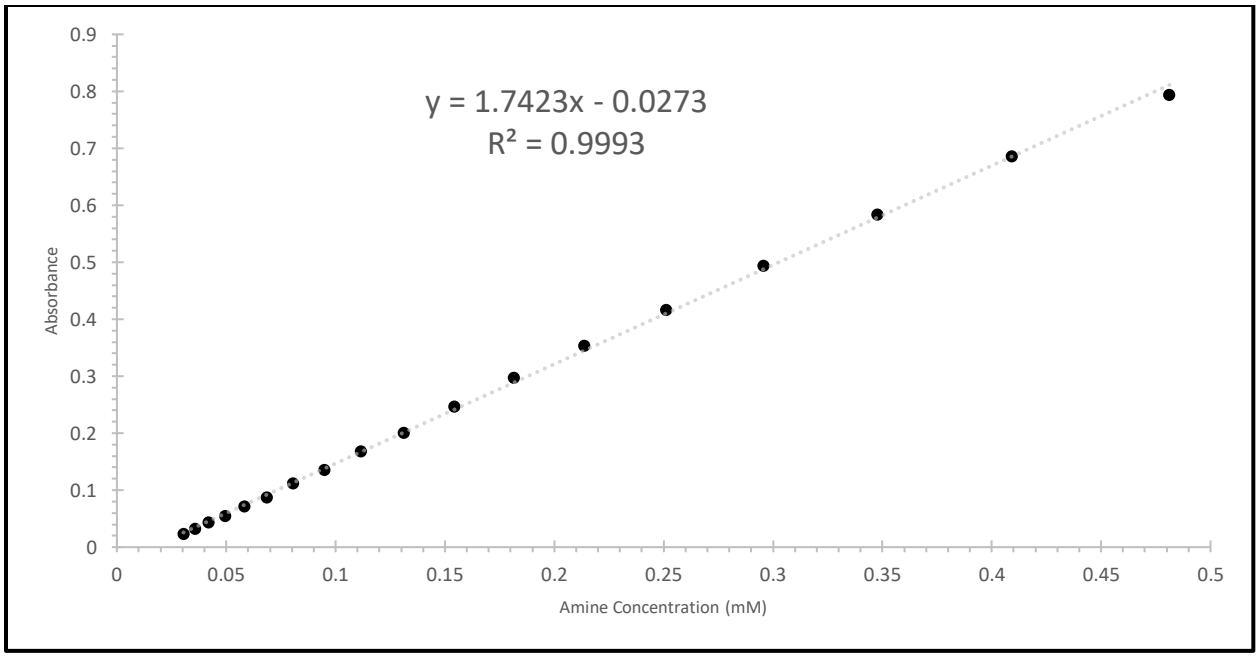

Figure S3. Calibration curve for primary amine concentration

Calibration curve to determine amine concentration in modified and unmodified gelatin was prepared using glycine standards in increasing concentrations and under identical conditions and OPA stock solution. A linear correlation with R^2=0.9993 was realized, following Beer-Lambert law.